J Arid Land (2023) 15(10): 1231–1244
https://doi.org/10.1007/s40333-023-0108-2

Science Press Springer-Verlag

Nitrogen application levels based on critical nitrogen absorption regulate processing tomatoes productivity, nitrogen uptake, nitrate distributions, and root growth in Xinjiang, China

JING Bo[1,2], SHI Wenjuan[2], DIAO Ming[1*]

[1] Key Laboratory of Special Fruits and Vegetables Cultivation Physiology and Germplasm Resources Utilization of Xinjiang Production and Construction Corps, Department of Horticulture, Agricultural College, Shihezi University, Shihezi 832003, China;

[2] State Key Laboratory of Eco-hydraulics in Northwest Arid Region of China, Xi'an University of Technology, Xi'an 710048, China

Abstract: The unreasonable nitrogen (N) supply and low productivity are the main factors restricting the sustainable development of processing tomatoes. In addition, the mechanism by which the N application strategy affects root growth and nitrate distributions in processing tomatoes remains unclear. In this study, we applied four N application levels to a field (including 0 (N0), 200 (N200), 300 (N300), and 400 (N400) kg/hm²) based on the critical N absorption ratio at each growth stage (planting stage to flowering stage: 22%; fruit setting stage: 24%; red ripening stage: 45%; and maturity stage: 9%). The results indicated that N300 treatment significantly improved the aboveground dry matter (DM), yield, N uptake, and nitrogen use efficiency (NUE), while N400 treatment increased nitrate nitrogen (NO_3^--N) residue in the 20–60 cm soil layer. Temporal variations of total root dry weight (TRDW) and total root length (TRL) showed a single-peak curve. Overall, N300 treatment improved the secondary root parameter of TRDW, while N400 treatment improved the secondary root parameter of TRL. The grey correlation coefficients indicated that root dry weight density (RDWD) in the surface soil (0–20 cm) had the strongest relationship with yield, whereas root length density (RLD) in the middle soil (20–40 cm) had a strong relationship with yield. The path model indicated that N uptake is a crucial factor affecting aboveground DM, TRDW, and yield. The above results indicate that N application levels based on critical N absorption improve the production of processing tomatoes by regulating N uptake and root distribution. Furthermore, the results of this study provide a theoretical basis for precise N management.

Keywords: critical N absorption; nitrogen use efficiency (NUE); beta model; total root dry weight (TRDW); root growth; processing tomato

Citation: JING Bo, SHI Wenjuan, DIAO Ming. 2023. Nitrogen application levels based on critical nitrogen absorption regulate processing tomatoes productivity, nitrogen uptake, nitrate distributions, and root growth in Xinjiang, China. Journal of Arid Land, 15(10): 1231–1244. https://doi.org/10.1007/s40333-023-0108-2

1 Introduction

Globally, the use of nitrogen (N) fertiliser has contributed to alleviating the problem of food security, particularly in realising high crop yields (Wang et al., 2018; Matiwane et al., 2019).

*Corresponding author: DIAO Ming (E-mail: diaoming@shzu.edu.cn)
The second and third authors contributed equally to this work.
Received 2023-02-27; revised 2023-07-13; accepted 2023-07-25

China is one of the countries with the largest N application in the world, the unreasonable application of N fertiliser is prevalent (Li and Lin, 2021). However, increasing the input of N fertiliser is unlikely to increase yield sustainably due to the decline in nitrogen use efficiency (NUE) (Liu et al., 2019; Liang et al., 2020). Moreover, blind N application leads to soil acidification and groundwater pollution in farmlands (Xiang et al., 2007; Gu et al., 2019). Therefore, it has become imperative for sustainable agricultural development to adopt scientific N fertiliser application practices, improve NUE, and reduce N fertiliser pollution in the environment (Li and Lin, 2021).

Critical N absorption is an important parameter for evaluating NUE in certain growth periods (Ulrich, 1952). In studies conducted in pastures without N limitation, the relationship between critical N concentration and aboveground dry matter (DM) has been established. The critical N concentration was defined after continuous verification and parameter modification and has been applied to most C3 and C4 plants (Greenwood et al., 1990; Wang et al., 2013). Through N nutrition diagnosis, field application rates of 240–320 kg/hm^2 N have been shown to satisfy rice plant growth (Ata-Ul-Karim et al., 2014). Although the critical N concentration model provides the total N application rates, the critical N application rates at each growth stage have not been implemented in agricultural practice. Therefore, the key to accurate N application is to determine the N application rates at each growth stage based on the critical N concentration model.

Processing tomato is among the vegetable crops with large cultivation areas globally (Farneselli et al., 2015) and contains important nutrients the human body requires (Lu et al., 2019). China has become a major producer and supplier of processing tomatoes, second only to the United States (Elia and Conversa, 2012). In recent years, drip irrigation technology has developed rapidly in China, significantly impacting the root architecture of processing tomatoes compared with traditional flood irrigation (Wang et al., 2022). Combined with the advantages of drip irrigation under mulch, the coupling mechanism of N absorption and the plant growth of processing tomatoes is vital for dryland agriculture development (Zotarelli et al., 2009; Li et al., 2016; Kang et al., 2017).

The spatial distribution of plant roots plays a crucial role in soil–shoot–atmosphere interactions (Liu et al., 2018). Soil nutrients and moisture become heterogeneous due to the interaction between roots, which impacts the community structure and composition (Day et al., 2003). Conversely, the spatial distribution of roots responds differently to soil nutrient and moisture conditions (Sun et al., 2018). For example, studies have shown that soil moisture altered root architecture and biomass of soybean (Fenta et al., 2014), while N deficiency resulted in notable changes in lateral roots of cotton (Zhu et al., 2022). In this study, we assume that the N application strategy improves the productivity of processing tomatoes by regulating root growth and nitrate distribution. Under drip irrigation under mulch, critical N absorption of processing tomatoes was used to calculate the critical N demand at each growth stage (Tei et al., 2002). Therefore, this research aimed to (1) investigate the effects of N application levels on the productivity of processing tomatoes, N absorption, and nitrate nitrogen (NO_3^--N) residue; (2) explore the dynamic root distribution of processing tomatoes under different N application levels; and (3) clarify the regulatory mechanism of N application based on critical N absorption model on the productivity and root distribution of processing tomatoes.

2 Materials and methods

2.1 Experiment site

The field experiment was conducted from April 2018 to July 2019 at the agricultural experimental station of Shihezi University (44°21′N, 86°04′E; 450 m) in Shihezi City, Xinjiang Uygur Autonomous Region of China. The precipitation was 76 and 114 mm during the growing season of processing tomatoes in 2018 and 2019, respectively, mainly concentrated in May. The average daily temperatures during growing season in 2018 and 2019 were 24.5°C and 23.1°C, respectively (Fig. 1). The chemical properties of topsoil (0–40 cm) were shown in Table 1.

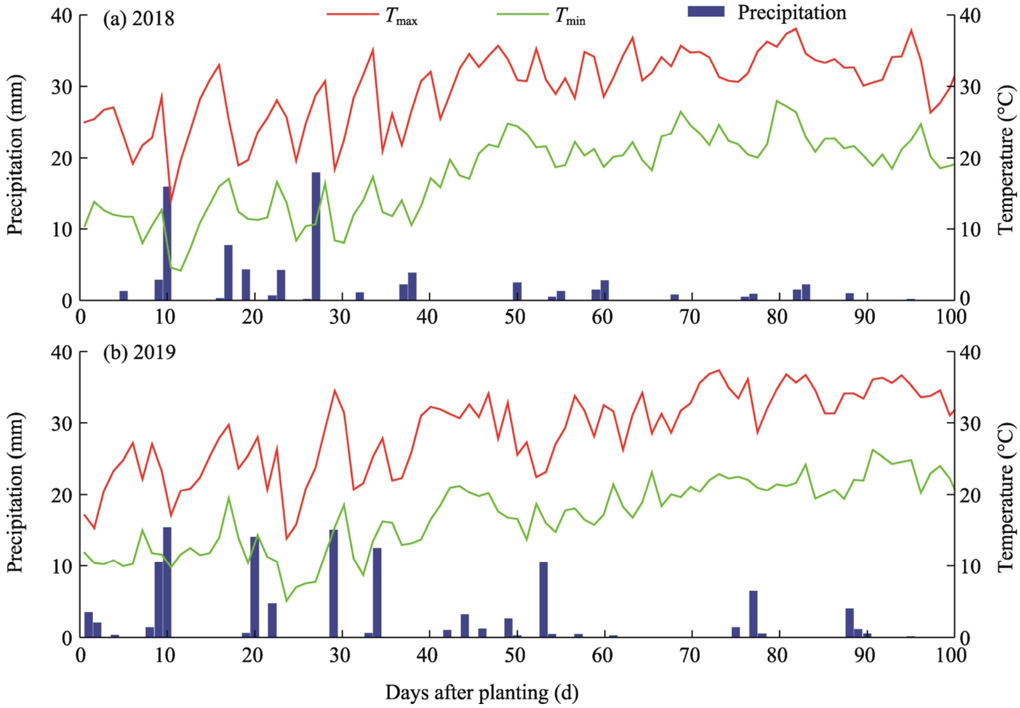

Fig. 1 Daily precipitation, maximum temperature (T_{max}), and minimum temperature (T_{min}) during the growing season of processing tomatoes in 2018 (a) and 2019 (b)

Table 1 Initial chemical properties of topsoil (0–40 cm) in 2018 and 2019

Year	pH	Total N (g/kg)	Available P (g/kg)	Available K (g/kg)	Organic matter (g/kg)
2018	7.53	0.85	0.02	0.34	10.12
2019	7.50	0.76	0.02	0.26	12.35

Note: N, nitrogen; P, phosphorus; K, potassium.

2.2 Experimental design and field management

Wang et al. (2013) developed a statistical method for constructing the critical N concentration dilution curve of processing tomatoes based on DM in northern Xinjiang. The critical N concentration dilution curve was calculated as follows:

$$\mathrm{Nc} = 4.352\mathrm{DM}^{-0.274}, \tag{1}$$

where Nc is the N concentration (%).

Critical N uptake was calculated by the following formula:

$$\mathrm{Nupt} = 43.521\mathrm{DM}^{0.726}, \tag{2}$$

where Nupt is the N uptake (kg/hm^2). The proportion of the N application rate at each growth stage to the total N application rate was determined using N uptake (Jing et al., 2020). We calculated the increase in N uptake at each growth stage according to the increase in DM of processing tomatoes at that specific stage, representing an increase in the critical N application rate. Therefore, the proportion of the N application rate at each growth stage to the total N application rate in the entire growth period was determined as follows: planting stage to flowering stage: 22%; fruit setting stage: 24%; red ripening stage: 45%; and maturity stage: 9%.

The experiment followed a completely randomised block design with three replicates. We set four N application levels, including 0, 200, 300, and 400 kg/hm^2 (i.e., N0, N200, N300, and N400, respectively). We used N fertiliser as the top dressing based on the proportion for each growth stage. Additionally, 210 kg/hm^2 of phosphate fertiliser and 150 kg/hm^2 of potassium fertiliser were simultaneously applied to the soil as base fertilisers.

Before the experiment, healthy seeds of processing tomatoes (Rieger 87-5) were sown in pots and provided with sufficient water. The seedlings were transplanted to the field on 29 April 2018 and 26 April 2019, when four true leaves appeared. The arrangement of the drip lines was set as 'one mulch, two drip lines, and two rows of processing tomatoes', with a plant spacing of 30 cm and a row spacing of 60 cm (Fig. 2). The area of each experimental plot was 86.4 m^2 (7.2 m×12.0 m). Irrigation was performed every 7 to 10 d, and each irrigation was controlled using a water meter. Irrigation was postponed in the event of rainfall. The total irrigation volume during the entire growth period was approximately 4700 m^3/hm^2.

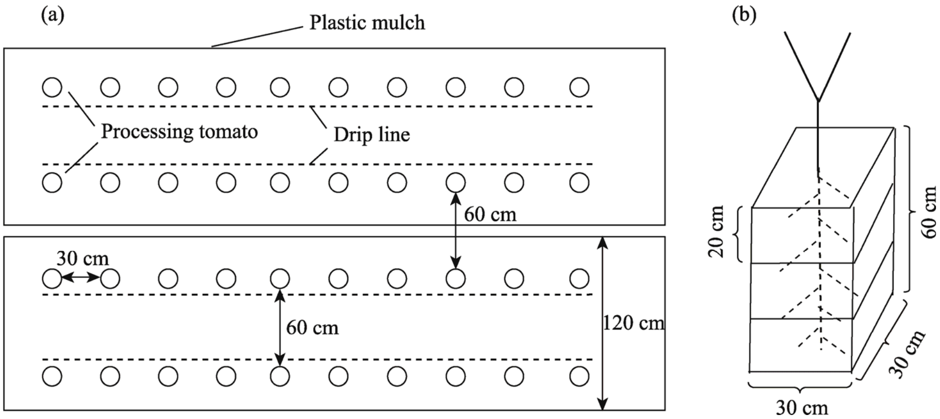

Fig. 2 (a), overhead view of the planting pattern of processing tomatoes in the experimental field; (b), stereoscopic view of root samples taken using the layered-mining method

2.3 Sampling and measurements

2.3.1 Measurement of aboveground dry matter (DM), nitrogen (N) uptake, yield, and nitrogen use efficiency (NUE)

At the harvest of processing tomatoes in 2018 and 2019, three representative plants were randomly collected from each plot to determine aboveground DM and N uptake. The aboveground parts of the plants were divided and oven-dried at 75°C to a constant weight, and aboveground DM was determined through gravimetry. Subsequently, the oven-dried plant samples were pulverised and screened through a 0.1 mm sieve. An appropriate amount of fine powder was digested with H_2SO_4-H_2O_2 to determine N concentration using the Kjeldahl method. N uptake was calculated as the product of DM and N concentration. The processing tomatoes were manually harvested from a 2.4 m^2 area per plot to determine yield. NUE (%) was calculated as follows:

$$\mathrm{NUE} = \frac{C_N - C_0}{Na} \times 100\%\ , \tag{3}$$

where C_N is the N uptake by plant in the areas where N is applied (kg/hm^2); C_0 is the N uptake by plant in the areas without N application (kg/hm^2); and Na is the application amount of N fertiliser (kg/hm^2).

2.3.2 Soil nitrate nitrogen (NO_3^--N) content

After the harvest of processing tomatoes, soil samples were collected from 0–80 cm layers at 20 cm intervals using an earth drill with a 2.5 cm diameter. The soil samples were dried at room temperature, and then milled and screened. The NO_3^--N content was determined using a 1 mol/L KCl solution through the ultraviolet spectrophotometer method.

2.3.3 Root sampling and analysis

In each plot, the roots of processing tomatoes were regularly harvested using the excavation method. Because the roots were mainly distributed in the 0–60 cm soil layer, and 30 cm around the plant was the concentration area of water and nutrients under drip irrigation (Jing et al., 2021),

the roots were collected in a soil column (30 cm×30 cm×60 cm) at 20 cm intervals (Fig. 2b). The root samples were obtained using the manual flushing method and scanned with a special root scanner (Epson Perfection V700 Photo, EPSON, Nagano, Japan). The root length was determined by analysing the scanned images using the Winrhizo Pro Vision 5.0 analysis program. Finally, the root samples were dried at 75°C for 12 h to obtain the root dry weight.

Root dry weight and root length per soil layer in the unit area were expressed by the following formulas:

$$\mathrm{RDW} = \frac{D}{S}, \tag{4}$$

$$\mathrm{RL} = \frac{L}{S}, \tag{5}$$

where RDW is the root dry weight (g/m^2); D is the root dry weight per soil layer (g); S is the soil area (m^2); RL is the root length (m/m^2); and L is the root length per soil layer (m). Total root dry weight (TRDW; g/m^2) or total root length (TRL; m/m^2) was the sum of root dry weight or root length of each soil layer.

Similarly, root dry weight density as well as root length density in unit volume of soil were expressed by the following formulas:

$$\mathrm{RDWD} = \frac{D}{V}, \tag{6}$$

$$\mathrm{RLD} = \frac{L}{V}, \tag{7}$$

where RDWD is the root dry weight density (g/m^3); RLD is the root length density (m/m^3); and V is the soil volume (m^3).

2.3.4 Quantitative analysis of beta model

The beta function of the root growth rate can determine the relationship between growth rate and duration (Yin et al., 2002; Wang et al., 2014). The formula is as follow:

$$w = w_{\max}\left(\frac{t_e - t}{t_e - t_m}\right) \times \left(\frac{t}{t_e}\right)^{\frac{t_e}{t_e - t_m}},\ 0 \le t < 2t_e - t_m;\ 0 < t_m < t_e, \tag{8}$$

where w is the growth parameters of root (TRDW or TRL); t is the number of days after planting (d); $w_{\max}$ is the maximum growth parameters of root when it grows to t_e day (g/m^2 or m/m^2 for TRDW or TRL, respectively); and t_m is the number of days when the root growth rate reaches the maximum value (d).

The average rate of root growth (c_a; (g/m^2)·d^{-1} or (m/m^2)·d^{-1} for TRDW or TRL, respectively) was expressed by the following formula:

$$c_a = \frac{w_{\max}}{t_e}. \tag{9}$$

The maximum root growth rate (c_m; (g/m^2)·d^{-1} or (m/m^2)·d^{-1} for TRDW or TRL, respectively) was expressed by the following formula (Yin et al., 2002):

$$c_m = \frac{2t_e - t_m}{t_e(t_e - t_m)} \times \left(\frac{t_m}{t_e}\right)^{\frac{t_m}{t_e - t_m}} \times w_{\max}. \tag{10}$$

2.3.5 Gray correlation

The gray correlation was evaluated by the method of Jia et al (2020):

Step 1: the original data transformation by equalization:

$$x'_{ij} = \frac{x_{ij}}{\bar{x}_j}, \tag{11}$$

where x'_{ij} is the equalized transformation value; x_{ij} is the actual value of index; and $\bar{x}_j$ the average value of index j.

Step 2: calculation of the correlation coefficient. The yield of processing tomatoes was used as the basic sequence, and the root growth parameters in each soil layer were set as the subsequence. The correlation coefficient was calculated by the following equation:

$$L_{0i}(K) = \frac{\Delta_{\min} + \rho\Delta_{\max}}{\Delta_{0i}(K) + \rho\Delta_{\max}}, \tag{12}$$

where $L_{0i}(K)$ is the correlation coefficient; $\Delta_{\min}$ and $\Delta_{\max}$ are the minimum and maximum values of the absolute differences at any moment, respectively; ρ is the resolution ratio, with the value set as 0.5; and $\Delta_{0i}(K)$ is the absolute difference between the two comparison sequences at moment K.

Step 3: correlation calculation. We used the following equation:

$$r_{0i} = \frac{1}{N}\sum_{K=1}^{N} L_{0i}(K), \tag{13}$$

where r_{0i} is the correlation between the subsequence i and the basic sequence; and N is the length of the comparison sequences.

Step 4: testing the significance of the correlation coefficient. The t value was calculated using the following equation:

$$t = \frac{r_{0i}}{1 - r_{0i}^2} \times \sqrt{n-2}, \tag{14}$$

where n–2 is the degree of freedom.

2.4 Statistical analyses

The analysis of variance was conducted using SPSS 17.0 software. Path analysis was employed to assess the relationships between indicators using SPSS 17.0 software. The least significant difference tests were used for significance analysis. Plotting was completed using Origin 9.0 software.

3 Results

3.1 Aboveground DM, yield, N uptake, and NUE under different N application levels

The N application levels significantly affected the aboveground DM, yield, N uptake, and NUE of processing tomatoes (P<0.01; Fig. 3). Although there were differences in the results between the two years due to climatic factors, the same trends were observed in different treatments for both years. The order of aboveground DM, yield, and N uptake for the four N application levels was ranked as N0<N200<N400<N300. Furthermore, NUE was higher under N300 treatment compared to N200 and N400 treatments.

3.2 Dynamic changes in total root dry weight (TRDW) and total root length (TRL)

The TRDW and TRL showed similar temporal variations in the two years (Fig. 4). The growth parameters of roots were fitted using the beta model, with the determination coefficients (R^2) exceeding 0.85, indicating that the beta model could effectively reflect root development. The growth process of roots under different N application levels showed a single-peak curve, characterised by slow growth, rapid growth, and then a gradual decline. There were differences in the TRDW and TRL under different N application levels (Table 2). During the two years, the order of the maximum growth parameters of root, the average rate of root growth, and the maximum root growth rate in TRDW for the four N application levels was N0<N200<N400<N300. Additionally, these values in TRL under N400 treatment were higher compared to other treatments.

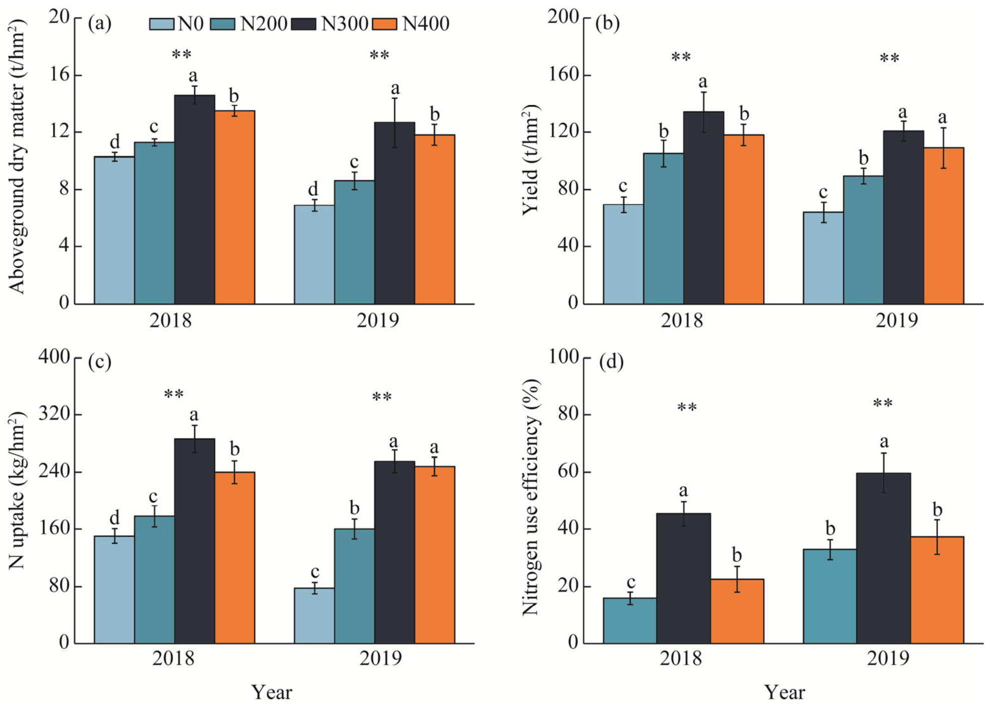

Fig. 3 Aboveground dry matter (DM; a), yield (b), nitrogen (N) uptake (c), and nitrogen use efficiency (NUE; d) under different N application levels in 2018 and 2019. N0, N200, N300, and N400 represent the N application levels of 0, 200, 300, and 400 kg/hm^2, respectively. Different lowercase letters in the same year indicate significant differences among different N application levels at P<0.05 level. ** indicates significance at P<0.01 level. Bars are standard errors.

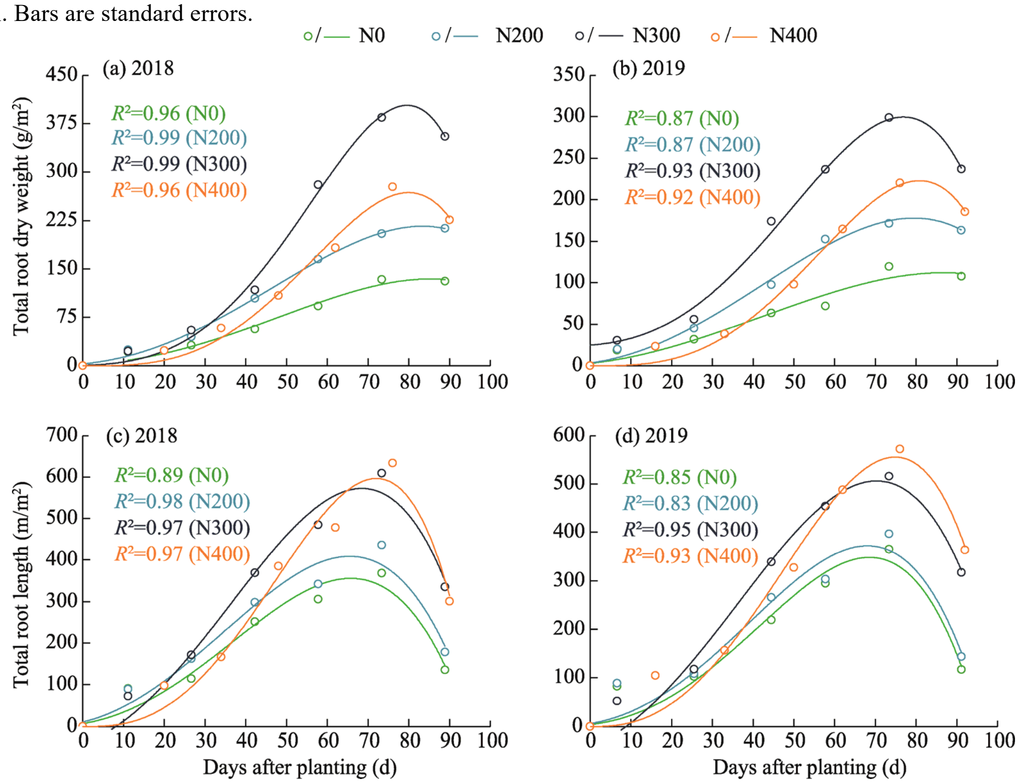

Fig. 4 Beta model of the variations in total root dry weight (TRDW; a and b) and total root length (TRL; c and d) under different N application levels in 2018 and 2019. The fitting curves are the beta equation fitting curves of the N application levels at 0, 200, 300, and 400 kg/hm^2.

Table 2 Secondary root parameters under different N application levels

Year	Root parameter	N application level	Secondary root parameter				
			w_{max} (g/m^2 or m/m^2)[#]	t_e (d)	t_m (d)	c_a ((g/m^2)•d^{-1} or (m/m^2)•d^{-1})[##]	c_m ((g/m^2)•d^{-1} or (m/m^2)•d^{-1})[##]
2018	TRDW	N0	134.34[d]	86.62[a]	53.80[c]	1.55[d]	2.59[d]
		N200	216.16[c]	84.99[b]	52.25[c]	2.54[c]	4.21[c]
		N300	403.28[a]	81.60[c]	60.47[a]	4.94[a]	10.19[a]
		N400	267.95[b]	79.90[c]	56.45[b]	3.35[b]	6.40[b]
	TRL	N0	355.76[c]	69.16[a]	43.05[b]	5.14[c]	8.59[c]
		N200	408.77[b]	68.93[a]	41.14[b]	5.91[b]	9.61[b]
		N300	581.57[a]	71.61[a]	42.61[b]	8.12[a]	13.14[a]
		N400	596.53[a]	72.02[a]	47.24[a]	8.28[a]	14.48[a]
2019	TRDW	N0	112.07[d]	88.03[a]	47.97[b]	1.27[d]	1.97[d]
		N200	177.91[c]	81.47[b]	48.42[b]	2.02[bc]	3.53[c]
		N300	308.10[a]	79.61[b]	57.08[a]	3.87[a]	7.55[a]
		N400	222.65[b]	80.83[b]	56.17[a]	2.75[b]	5.14[ab]
	TRL	N0	348.19[d]	71.68[a]	47.20[a]	5.36[b]	8.53[b]
		N200	371.98[c]	71.23[a]	45.19[a]	5.22[b]	8.86[b]
		N300	514.03[b]	73.25[a]	42.58[b]	7.02[a]	11.20[a]
		N400	555.99[a]	74.85[a]	47.21[a]	7.43[a]	12.54[a]

Note: N0, N200, N300, and N400 represent the N application levels of 0, 200, 300, and 400 kg/hm^2, respectively. TRDW, total root dry weight; TRL, total root length; w_{max}, the maximum growth parameters of root; t_e, the number of days when the root growth parameter reaches the maximum value; t_m, the number of days when the root growth rate reaches the maximum value; c_a, the average rate of root growth; c_m, the maximum root growth rate. Different lowercase letters in the same year indicate significant differences among different N application levels at P<0.05 level. [#] represents that the unit of w_{max} is g/m^2 for TRDW and m/m^2 for TRL; [##] represents that the unit of c_a and c_m is (g/m^2)•d^{-1} for TRDW and (m/m^2)•d^{-1} for TRL.

3.3 Soil NO_3^--N content, root dry weight density (RDWD), and root length density (RLD) in soil profiles

At the harvest stage, the soil NO_3^--N content showed an initial increase followed by a decrease with an increase in soil depth under all treatments (Fig. 5). The order of the total soil NO_3^--N content for the four N application levels was N0<N200<N300<N400. Remarkably, N400 treatment resulted in a significant accumulation of soil NO_3^--N content in the 20–60 cm soil layer. In addition, the vertical distribution of the roots showed adaptive changes. Both RDWD and RLD decreased gradually with an increase in soil depth (Fig. 6). The root was mainly distributed in the 0–20 cm soil layer. Within the 0–20 cm soil layer, the order of RDWD and RLD under the four N

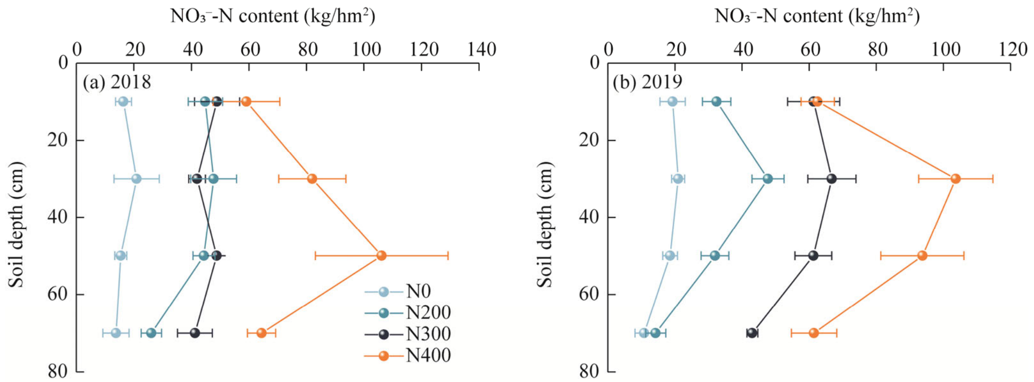

Fig. 5 Soil nitrate nitrogen (NO_3^--N) content in the 0–80 cm soil layers under different N application levels in 2018 (a) and 2019 (b). Bars are standard errors.

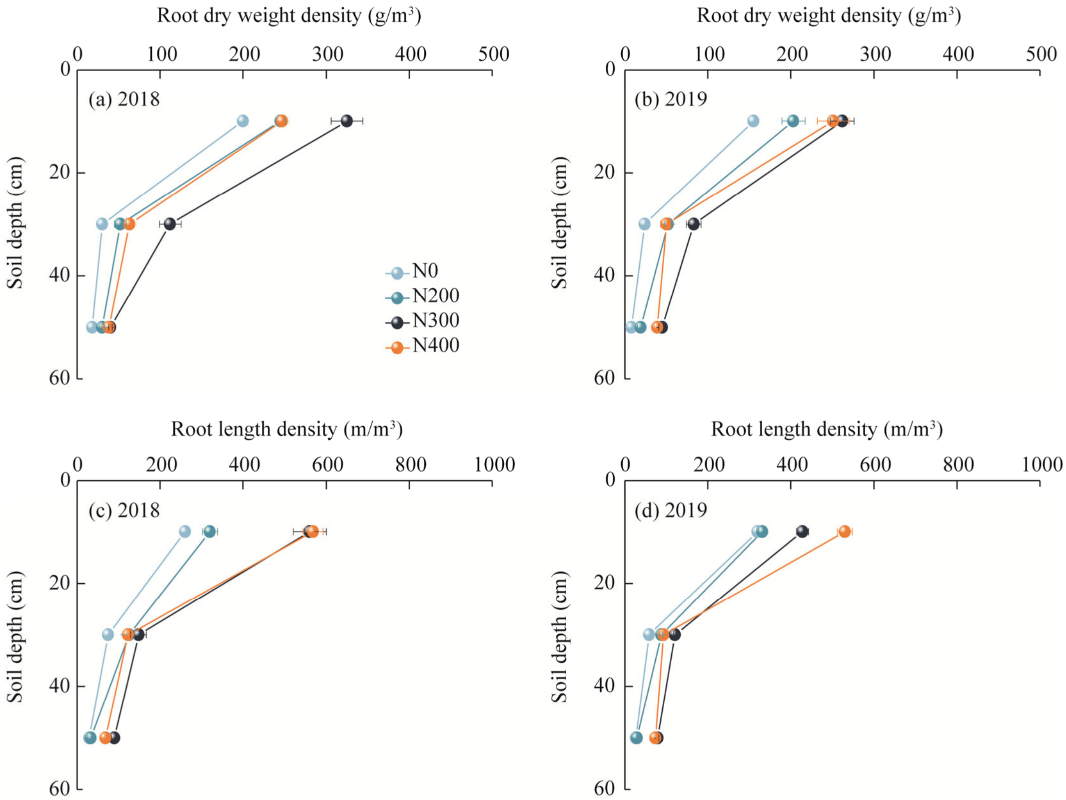

Fig. 6 Changes in root dry weight density (RDWD; a and b) and root length density (RLD; c and d) in different soil layers under different N application levels in 2018 and 2019. Bars are standard errors.

application levels was N0<N200<N400<N300 and N0<N200<N300<N400, respectively. In the 20–40 and 40–60 cm soil layers, the RDWD and RLD under N300 treatment were higher compared to other treatments.

3.4 Grey correlation coefficients between yield and root density in different soil layers

Under N application levels based on critical N absorption, the minimum grey correlation coefficient between yield and RDWD or RLD was observed in the 40–60 cm soil layer. The maximum grey correlation coefficient between yield and RDWD was found in the 0–20 cm soil layer, while the maximum grey correlation coefficient between yield and RLD was observed in the 20–40 cm soil layer (Table 3). Additionally, N application levels affected the grey correlation coefficient in the 0–60 cm soil layer. For RDWD, the grey correlation coefficient of N300 treatment was higher than that of other treatments in different soil layers. For RLD, the grey correlation coefficient of N400 treatment was higher than that of other treatments in the 0–20 and 40–60 cm soil layers, while the grey correlation coefficient of N0 treatment was higher than that of other treatments in the 20–40 cm soil layer. These results indicated that RDWD in the surface soil (0–20 cm) had the strongest relationship with yield, but its influence decreased with increasing soil depth. The RLD in the 20–40 cm soil layer also had a strong relationship with yield, significantly impacting yield under N deficiency (P<0.05).

3.5 Path analysis of aboveground DM, TRDW, N uptake, soil NO_3^--N content, and yield

The path analysis model was used to assess the relationships among aboveground DM, TRDW, N uptake, soil NO_3^--N content, and yield (Fig. 7). The direct impact degree on yield followed the order of N uptake>TRDW>aboveground DM>soil NO_3^--N content. Moreover, the coefficients of N uptake and TRDW on yield were significant (P<0.01). N uptake significantly and positively affected TRDW and aboveground DM (P<0.05). In addition, aboveground DM and soil NO_3^--N

content were negatively related to yield. These findings indicated that an increase in nutrient growth and soil N does not necessarily translate into continuous yield improvement and may result in plant overgrowth and N leaching.

Table 3 Grey correlation coefficients between root parameters in different soil layers with yield under different N application levels

Root parameter	N application level	Soil depth (cm)					
		2018			2019		
		0–20	20–40	40–60	0–20	20–40	40–60
RDWD (g/m^3)	N0	0.649*	0.536	0.494	0.614	0.548	0.599
	N200	0.651*	0.501	0.515	0.729**	0.544	0.587
	N300	0.685	0.645	0.595	0.759*	0.677	0.657
	N400	0.635	0.534	0.478	0.693	0.549	0.523
RLD (m/m^3)	N0	0.559	0.859**	0.557	0.641	0.727*	0.554
	N200	0.573	0.676	0.508	0.583	0.637	0.540
	N300	0.553	0.559	0.581	0.499	0.576	0.481
	N400	0.673	0.757*	0.610	0.671	0.726	0.663

Note: RDWD and RLD are root dry weight density and root length density, respectively. * and ** indicate significant correlation coefficient at P<0.05 and P<0.01 levels, respectively.

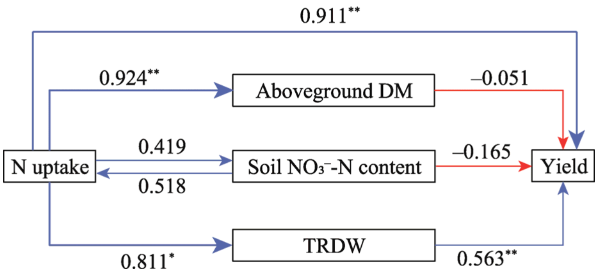

Fig. 7 Path model among aboveground DM, TRDW, N uptake, soil NO_3^--N content, and yield. Blue lines represent positive relationships, while red lines represent negative relationships. The width of the arrows represents the strength of significant standardised path coefficients. * and ** indicate significant path coefficient at P<0.05 and P<0.01 levels, respectively.

4 Discussion

4.1 Productivity and N uptake responses to various N application levels

Reasonable fertilisation plans have been proven effective in promoting aboveground DM and yield (Ronga et al., 2017; Banger et al., 2020). In this study, we implemented an N application strategy based on critical N absorption at each growth stage. Our results showed a positive correlation between N application rate and aboveground DM or yield of processing tomatoes within 300 kg N/hm^2. However, the 400 kg/hm^2 N application hindered aboveground DM and yield, consistent with the findings of Farneselli et al. (2018). This could be caused by the following reasons. First, an adequate N input ensures root growth and water absorption, thereby promoting aboveground DM and yield. However, excessive N input causes inorganic N accumulation in the soil, resulting in soil salinisation (Cheng et al., 2021). Second, high N concentration directly reduced soil microbial activity by enhancing specific ion toxicity, thereby inhibiting root growth and nutrient absorption (Yan et al., 2021).

Reasonable regulation of soil N holds considerable potential for maintaining stable yield and NUE in arid areas (Zheng et al., 2021). In this study, N300 treatment had the highest N uptake

and NUE, while N400 treatment had the highest soil NO_3^--N content. Despite the plastic film mulching increasing soil water storage, the high N concentration accelerated soil moisture reduction due to excessive vegetative growth and an increased transpiration rate (Long et al., 2021). Therefore, under water-deficit conditions, the migration rate of NO_3^--N to deep soil could be slower in N400 treatment. In addition, high N concentration inhibits plant N uptake and increases NO_3^--N residue (Yuan et al., 2018).

4.2 Root growth responses to various N application levels

In this study, the secondary root parameters were analysed using the beta model. Overall, compared with N0 and N200 treatments, N300 treatment improved the secondary root parameter of TRDW, while N400 treatment improved the secondary root parameter of TRL. Wang et al. (2014) reported that the community structures of crops were optimised by maintaining high TRDW in the late growth period under a reasonable planting mode. These improvements may be due to nutrient deficiency under N0 and N200 treatments, which led to decreased soil microbial activity and hindered root growth (Isobe et al., 2018). In addition, nutrient deficiency in the late growth period led to the blockage of plant physiological metabolism (Zaman et al., 2021). Most roots of processing tomatoes were accumulated in the uppermost (0–20 cm) soil layer. Generally, plant root configuration is controlled by genetic factors (Clark et al., 2011; Ning et al., 2019). However, plant roots exhibit adaptive changes in response to specific environmental conditions in highly distinct growth environments (Martins et al., 2019).

Appropriate N concentration promoted root growth (Hackett, 1972; Drew, 1975; Postma et al., 2014), while high N concentration inhibited it (Forde and Lorenzo, 2001). This phenomenon was also observed in different soil layers in this study. Specifically, the RDWD of N300 treatment was highest compared to other treatments in the 0–20 cm soil layer, while the RLD of N400 treatment was the largest. This could be attributed to the following two mechanisms. First, high N concentration inhibits the biosynthesis and transport of indole acetic acid, thereby inhibiting taproot growth (Walch-liu et al., 2001). Second, lateral root growth is hindered by the inhibition of dividing tissue activity (Zhang and Forde, 1998). Additionally, research has shown that high N concentration promotes the regeneration of superficial capillary roots, which may explain the longer root length in the topsoil of N400 treatment. In this study, the RLD of N300 treatment was highest compared to other treatments in the 40–60 cm soil layer. Remarkably, the increased RLD in the deeper soil layer effectively facilitated nutrient and water absorption (Zhang et al., 2009; Jia et al., 2020).

4.3 Crucial determinants of promotion in productivity

N is essential for normal plant metabolism and is the main limiting factor for crop yields (Shi et al., 2022). The distribution of carbohydrates among various plant organs ensures a balanced growth ratio between underground and aboveground parts, but applying N fertilisers can disrupt this growth balance (Lovelli et al., 2012). Thus, N fertilisers significantly affect the biomass of plant shoots and roots (Sainju et al., 2017). Furthermore, N fertilisation plays a crucial role in soil pore structure and microbial balance (Liang and Shi, 2021). Therefore, employing the path model is necessary to understand the relationships among N uptake, aboveground DM, TRDW, soil NO_3^--N content, and yield. The present path model indicated that N uptake is a crucial factor affecting aboveground DM, TRDW, and yield. Moreover, aboveground DM and soil NO_3^--N content were negatively related to yield, suggesting increased vegetative growth and the risk of NO_3^--N leaching. Notably, no significant negative correlation was observed between aboveground DM and yield, mainly due to the vigorous nutritional growth of plants under N400 treatment. However, N300 treatment obtained the highest yield. According to the nutrient status of the soil and plants, plants use specialised vascular tissue to transport N, effectively regulating biomass distribution (Hermans et al., 2006; Litton et al., 2007; McCarthy and Enquist, 2007). However, due to the soil water infiltration caused by rainfall and irrigation, N leaching was inevitable (Wang and Li, 2019). In conclusion, we confirmed the crucial role of N application

based on critical N absorption in improving productivity, although the risk of NO_3^--N leaching still exists. Moreover, further validation is needed to understand the physiological mechanisms underlying the responses of processing tomatoes to critical N absorption.

5 Conclusions

Under N application levels based on critical N absorption, N300 treatment significantly improved the productivity and NUE of processing tomatoes, while N400 treatment increased the risk of NO_3^--N leaching. The roots under N300 and N400 treatments showed increased growth, which promoted yield. While the RDWD in the surface soil (0–20 cm) had the strongest relationship with yield, the RLD in the middle soil (20–40 cm) also had a strong relationship with yield. Additionally, N uptake was a crucial factor influencing aboveground DM, TRDW, and yield. Our results suggested that the 300 kg/hm^2 N application, based on the critical N absorption ratio (planting stage to flowering stage: 22%; fruit setting stage: 24%; red ripening stage: 45%; and maturity stage: 9%), improved root distribution and soil NO_3^--N content and promoted the productivity processing tomatoes.

Conflict of interest

The authors declare that they have no known competing financial interests or personal relationships that could have appeared to influence the work reported in this paper.

Acknowledgements

This research was supported by the National Natural Science Foundation of China (42077011).

Author contributions

Conceptualization: DIAO Ming, SHI Wenjuan; Data curation: JING Bo; Methodology: DIAO Ming, SHI Wenjuan; Investigation: DIAO Ming; Formal analysis: JING Bo; Writing - original draft preparation: JING Bo; Writing - review and editing: DIAO Ming, SHI Wenjuan; Funding acquisition: DIAO Ming, SHI Wenjuan; Resources: DIAO Ming; Supervision: DIAO Ming; Project administration: DIAO Ming.

References

Ata-Ul-Karim S T, Zhu Y, Yao X, et al. 2014. Determination of critical nitrogen dilution curve based on leaf area index in rice. Field Crops Research, 167: 76–85.

Banger K, Wagner-Riddle C, Grant B B, et al. 2020. Modifying fertilizer rate and application method reduces environmental nitrogen losses and increases corn yield in Ontario. Science of The Total Environment, 722: 137851, doi: 10.1016/j. scitotenv. 2020.137851.

Cheng M H, Wang H D, Fan J L, et al. 2021. Effects of nitrogen supply on tomato yield, water use efficiency and fruit quality: A global meta-analysis. Scientia Horticulturae, 290: 110553, doi: 10.1016/j.scienta.2021.110553.

Clark R T, MacCurdy R B, Jung J K, et al. 2011. Three-dimensional root phenotyping with a novel imaging and software platform. Plant Physiology, 156(2): 455–465.

Day K J, John E A, Hutchings M J. 2003. The effects of spatially heterogeneous nutrient supply on yield, intensity of competition and root placement patterns in *Briza media* and *Festuca ovina*. Functional Ecology, 17(4): 454–463.

Drew M C. 1975. Comparison of the effects of a localized supply of phosphate, nitrate, ammonium and potassium on the growth of the seminal root system, and the shoot, in barley. New Phytologist, 75(3): 479–490.

Elia A, Conversa G. 2012. Agronomic and physiological responses of a tomato crop to nitrogen input. European Journal of Agronomy, 40: 64–74.

Farneselli M, Benincasa P, Tosti G, et al. 2015. High fertigation frequency improves nitrogen uptake and crop performance in processing tomato grown with high nitrogen and water supply. Agricultural Water Management, 154: 52–58.

Farneselli M, Tosti G, Onofri A, et al. 2018. Effects of N sources and management strategies on crop growth, yield and potential N leaching in processing tomato. European Journal of Agronomy, 98: 46–54.

Fenta B A, Beebe S E, Kunert K J, et al. 2014. Field phenotyping of soybean roots for drought stress tolerance. Agronomy Journal, 4(3): 418–435.

Forde B, Lorenzo H. 2001. The nutritional control of root development. Plant and Soil, 232: 51–68.

Greenwood D J, Lemaire G, Gosse G, et al. 1990. Decline in percentage N of C_3 and C_4 crops with increasing plant mass. Annals of Botany, 66(4): 425–436.

Gu X B, Cai H J, Zhang Z T, et al. 2019. Ridge-furrow full film mulching: An adaptive management strategy to reduce irrigation of dryland winter rapeseed (*Brassica napus* L.) in northwest China. Agricultural and Forest Meteorology, 266–267: 119–128.

Hackett C. 1972. A method of applying nutrients locally to roots under controlled conditions, and some morphological effects of locally applied nitrate on the branching of wheat roots. Australian Journal of Biological Sciences, 25(6): 1169–1180.

Hermans C, Hammond J P, White P J, et al. 2006. How do plants respond to nutrient shortage by biomass allocation? Trends in Plant Science, 11(12): 610–617.

Isobe K, Oka H, Watanabe T, et al. 2018. High soil microbial activity in the winter season enhances nitrogen cycling in a cool-temperate deciduous forest. Soil Biology & Biochemistry, 124: 90–100.

Jia Q M, Yang L Y, An H Y, et al. 2020. Nitrogen fertilization and planting models regulate maize productivity, nitrate and root distributions in semi-arid regions. Soil & Tillage Research, 200: 104636, doi: 10.1016/j.still.2020.104636.

Jing B, Niu N, Zhang W L, et al. 2020. ^{15}N tracer-based analysis of fertiliser nitrogen accumulation, utilisation and distribution in processing tomato at different growth stages. Acta Agriculturae Scandinavica Section B-Soil and Plant Science, 70(8): 620–627.

Jing B, Niu N, Zhang W L, et al. 2021. Effects of different nitrogen application rates on root architecture of processing tomatoes. Journal of Drainage and Irrigation Machinery Engineering, 39(12): 1257–1263. (in Chinese).

Kang S Z, Hao X M, Du T S, et al. 2017. Improving agricultural water productivity to ensure food security in China under changing environment: From research to practice. Agricultural Water Management, 179: 5–17.

Li J, Lin W F. 2021. Effects of nitrogen fertilizer rates on the growth and nutrient utilization of calla lily intercropped with rubber trees. Soil & Tillage Research, 211: 105031, doi: 10.1016/j.still.2021.105031.

Li X L, Zhang X T, Niu J, et al. 2016. Irrigation water productivity is more influenced by agronomic practice factors than by climatic factors in Hexi Corridor, Northwest China. Scientific Reports, 6: 37971, doi: 10.1038/srep37971.

Liang J P, He Z J, Shi W J. 2020. Cotton/mung bean intercropping improves crop productivity, water use efficiency, nitrogen uptake, and economic benefits in the arid area of Northwest China. Agricultural Water Management, 240: 106227, doi: 10.1016/j.agwat.2020.106277.

Liang J P, Shi W J. 2021. Poly-γ-glutamic acid improves water-stable aggregates, nitrogen and phosphorus uptake efficiency, water-fertilizer productivity, and economic benefit in barren desertified soils of Northwest China. Agricultural Water Management, 245: 106551, doi: 10.1016/j.agwat.2020.106551.

Litton C M, Raich J W, Ryan M G. 2007. Carbon allocation in forest ecosystems. Global Change Biology, 13: 2089–2109.

Liu W X, Ma G, Wang C Y, et al. 2018. Irrigation and nitrogen regimes promote the use of soil water and nitrate nitrogen from deep soil layers by regulating root growth in wheat. Frontiers in Plant Science, 9: 32, doi: 10.3389/fpls.2018.00032.

Liu Z X, Gao F, Liu Y, et al. 2019. Timing and splitting of nitrogen fertilizer supply to increase crop yield and efficiency of nitrogen utilization in a wheat-peanut relay intercropping system in China. Crop Journal, 7(1): 101–112.

Long G Q, Li L H, Wang D, et al. 2021. Nitrogen levels regulate intercropping-related mitigation of potential nitrate leaching. Agriculture Ecosystems & Environment, 319: 107540, doi: 10.1016/j.agee.2021.107540.

Lovelli S, Scopa A, Perniola M, et al. 2012. Abscisic acid root and leaf concentration in relation to biomass partitioning in salinized tomato plants. Journal of Plant Physiology, 169: 226–233.

Lu J, Shao G C, Cui J T, et al. 2019. Yield, fruit quality and water use efficiency of tomato for processing under regulated deficit irrigation: A meta-analysis. Agricultural Water Management, 222: 301–312.

Ning S R, Chen C, Zhou B B, et al. 2019. Evaluation of normalized root length density distribution models. Field Crops Research, 242: 107604, doi: 10.1016/j.fcr.2019.107604.

Martins A O, Omena-Garcia R P, Oliveira F S, et al. 2019. Differential root and shoot responses in the metabolism of tomato plants exhibiting reduced levels of gibberellin. Environmental and Experimental Botany, 157: 331–343.

Matiwane S E, Aremu A O, Valentine A J, et al. 2019. Nutritional status of KwaZulu-Natal soils affects microbe symbiosis, nitrogen utilization and growth of *Vigna radiata* (L.) R. Walczak. South African Journal of Botany, 126: 115–120.

McCarthy M C, Enquist B J. 2007. Consistency between an allometric approach and optimal partitioning theory in global patterns of plant biomass allocation. Functional Ecology, 21(4): 713–720.

Postma J A, Dathe A, Lynch J P. 2014. The optimal lateral root branching density for maize depends on nitrogen and

phosphorus availability. Plant Physiology, 166(2): 590–602.

Ronga D, Zaccardelli M, Lovelli S, et al. 2017. Biomass production and dry matter partitioning of processing tomato under organic vs conventional cropping systems in a Mediterranean environment. Scientia Horticulturae, 224: 163–170.

Sainju U M, Allen B L, Lenssen A W, et al. 2017. Root biomass, root/shoot ratio, and soil water content under perennial grasses with different nitrogen rates. Field Crops Research, 210: 183–191.

Shi Z G, Wei F, Wan R, et al. 2022. Comprehensive evaluation of nitrogen use efficiency of different *Lycium barbarum* L. cultivars under nitrogen stress. Scientia Horticulturae, 295: 110807, doi: 10.1016/j.scienta.2021.110807.

Sun Y B, Bi H X, Xu H S, et al. 2018. Variation of fine roots distribution in apple (*Malus pumila* M.)-crop intercropping systems on the loess plateau of China. Agronomy Journal, 8(12): 1–16.

Tei F, Benincasa P, Guiducci M. 2002. Critical nitrogen concentration in processing tomato. European Journal Agronomy, 18(1–2): 45–55.

Ulrich A. 1952. Physiological bases for assessing the nutritional requirements of plants. Annual Review of Plant Physiology, 3(1): 207–228.

Walch-liu P, Neumann G, Engels C. 2001. Response of shoot and root growth to supply of different nitrogen forms is not related to carbohydrate and nitrogen status of tobacco plants. Journal of Plant Nutrition Soil Science, 164(1): 97–103.

Wang J W, Du Y D, Niu W Q, et al. 2022. Drip irrigation mode affects tomato yield by regulating root-soil-microbe interactions. Agricultural Water Management, 260: 107188, doi: 10.1016/j.agwat.2021.107188.

Wang X, Ma F Y, Diao M, et al. 2013. Simulation of critical nitrogen concentration, nitrogen absorption and nitrogen nutrition index of drip irrigation tomato. Transactions of the Chinese Society of Agricultural Engineering, 29(18): 99–108. (in Chinese).

Wang Y H, Hu W L, Zhang X L, et al. 2014. Effects of cultivation patterns on winter wheat root growth parameters and grain yield. Field Crops Research, 156: 208–218.

Wang Y, Zhu Y C, Zhang S X, et al. 2018. What could promote farmers to replace chemical fertilizers with organic fertilizers? Journal of Cleaner Production, 199: 882–890.

Wang Z H, Li S X. 2019. Nitrate N loss by leaching and surface runoff in agricultural land: A global issue (a review). Advances in Agronomy, 156: 159–217.

Xiang P A, Zhou Y, Huang H, et al. 2007. Discussion on the green tax stimulation measure of nitrogen fertilizer non-point source pollution control-taking the Dongting Lake area in China as a case. Agricultural Sciences in China, 6(6): 732–741.

Yan D Z, Long X E, Ye L L, et al. 2021. Effects of salinity on microbial utilization of straw carbon and microbial residues retention in newly reclaimed coastal soil. European Journal Soil Biology, 107: 103364, doi: 10.1016/j.ejsobi.2021.103364.

Yin X Y, Goudriaan J, Lantinga E A, et al. 2002. A flexible sigmoid function of determinate growth. Annals of Botany, 91(3): 361–371.

Yuan S N, Tan Z X, Huang Q Y. 2018. Migration and transformation mechanism of nitrogen in the biomass-biochar-plant transport process. Renewable & Sustainable Energy Reviews, 85: 1–13.

Zaman I, Ali M, Shahzad K, et al. 2021. Effect of plant spacings on growth, physiology, yield and fiber quality attributes of cotton genotypes under nitrogen fertilization. Agronomy Journal, 11: 2589, doi: 10.3390/agronomy11122589.

Zhang H, Forde B G. 1998. An Arabidopsis MADS box gene that controls nutrient-induced changes in root architecture. Science, 279: 407–409.

Zheng J, Fan J L, Zhang F C, et al. 2021. Interactive effects of mulching practice and nitrogen rate on grain yield, water productivity, fertilizer use efficiency and greenhouse gas emissions of rainfed summer maize in northwest China. Agricultural Water Management, 248: 106778, doi: 10.1016/j.agwat.2021.106778.

Zhu L X, Liu L T, Sun H C, et al. 2022. The responses of lateral roots and root hairs to nitrogen stress in cotton based on daily root measurements. Journal of Agronomy and Crop Science, 208(1): 89–105.

Zotarelli L, Scholberg J M, Dukes M D, et al. 2009. Tomato yield, biomass accumulation, root distribution and irrigation water use efficiency on a sandy soil, as affected by nitrogen rate and irrigation scheduling. Agricultural Water Management, 96(1): 23–34.